

This article was downloaded by:

On: 14 January 2011

Access details: *Access Details: Free Access*

Publisher *Taylor & Francis*

Informa Ltd Registered in England and Wales Registered Number: 1072954 Registered office: Mortimer House, 37-41 Mortimer Street, London W1T 3JH, UK



## **Molecular Simulation**

Publication details, including instructions for authors and subscription information:

<http://www.informaworld.com/smpp/title~content=t713644482>

### **Molecular dynamics simulation of thread break-up and formation of droplets in nanoejection system**

Chi-Fu Dai<sup>a</sup>; Rong-Yeu Chang<sup>a</sup>

<sup>a</sup> Department of Chemical Engineering, National Tsing-Hua University, Hsinchu, Taiwan, R.O.C

**To cite this Article** Dai, Chi-Fu and Chang, Rong-Yeu(2009) 'Molecular dynamics simulation of thread break-up and formation of droplets in nanoejection system', *Molecular Simulation*, 35: 4, 334 — 341

**To link to this Article:** DOI: 10.1080/08927020802430745

**URL:** <http://dx.doi.org/10.1080/08927020802430745>

PLEASE SCROLL DOWN FOR ARTICLE

Full terms and conditions of use: <http://www.informaworld.com/terms-and-conditions-of-access.pdf>

This article may be used for research, teaching and private study purposes. Any substantial or systematic reproduction, re-distribution, re-selling, loan or sub-licensing, systematic supply or distribution in any form to anyone is expressly forbidden.

The publisher does not give any warranty express or implied or make any representation that the contents will be complete or accurate or up to date. The accuracy of any instructions, formulae and drug doses should be independently verified with primary sources. The publisher shall not be liable for any loss, actions, claims, proceedings, demand or costs or damages whatsoever or howsoever caused arising directly or indirectly in connection with or arising out of the use of this material.

## Molecular dynamics simulation of thread break-up and formation of droplets in nanoejection system

Chi-Fu Dai\* and Rong-Yeu Chang

Department of Chemical Engineering, National Tsing-Hua University, Hsinchu, Taiwan, R.O.C

(Received 22 March 2008; final version received 25 August 2008)

This study investigated nanojet processes by a non-equilibrium molecular dynamics simulation. The phenomena of liquid thread break-up and droplet formation were simulated by compressing liquid propane molecules with various compressing velocities. Properties' distributions show that, at the nanoscale, density and pressure were neither uniform nor continuous during the ejection process. Shear heating phenomena were found in the contact area of the nozzle channel. A linear relationship between the length of liquid threads and the compressing velocity was also found in this study. The results from different trials using various compressing velocities show that higher compressing velocities in nanojet processes result in longer liquid thread lengths and liquid molecules with higher energy levels. Therefore, the ejection process is more unstable, resulting in an increase in the number of evaporating molecules and satellite droplets. Results that illustrate various features are presented to aid in the comprehension of the nanojet processes.

**Keywords:** simulation; molecular dynamics; nanojet ejection

### 1. Introduction

Inkjet printing is a promising technology. It can deliver micro-sized droplets into particular targets. Recently, with the progress of nanomachining, nanosized nozzles have been developed [1]; they are used in various applications at macro- and nanoscales [2], e.g. biomedical/chemical sample handling, fuel injection/mixing control, optical component fabrication and integration, solid free-forming, nanomanufacturing processes and so on.

The ejection phenomenon is influenced by the balance between surface tension and inertia. Although continuum mechanics is well accepted in describing the non-linear dynamics and free-surface jet flow at the macroscale [3], continuum modelling is not applicable when nanoscale or molecular-level physics becomes dominant. In addition to nanoscale experimental investigation, molecular dynamics (MD) simulation is a powerful tool to study nanoscale processes under different operating conditions.

Recently, many researchers have reported MD simulation results and theory for nanojet formation. Landman and Moseler [4] first presented MD simulation results for a 6-nm diameter nozzle with molecular propane as the confined fluid. They found that a jet can be formed with nozzle inlet pressures of 500 MPa and temperatures of 150 K. They suggested a stochastic hydrodynamic lubrication equation (SLE) [4,5] based on the Navier–Stokes equations with a Gaussian white noise distribution to describe the jet profile evolution. And based on the MD simulation results [4], Eggers [6] used self-similar profiles to describe the break-up mode and dynamics of liquid

nanojets. Choi et al. [7] reported on ejection behaviours of a nanojet with nozzles of various diameters. The results showed the effect of nozzle outlet size on the break-up time and on the growth rate of spherical droplets. Ichiki and Consta [8] reported on ejection processes with aqueous charged nanodroplets. Murad and Puri [9] reported on nanoscale jet collisions for various impact velocities and found that the duration between collision and recoil is dependent on impact velocity.

In the previously mentioned reports, some characteristics of nanojets have been pointed out. However, there are still many control factors that should be investigated to help us better understand the ejection process and the break-up mechanism. The break-up behaviour influences the formation of droplets and the existence of satellite droplets. Determining the break-up position will also help us in determining the distance between the nozzle and particular targets. This study used MD simulation to investigate the whole nanojet ejection process for various compressing velocities. A common fuel material, liquid propane, was used as the fluid in these ejection processes.

### 2. Simulation method and system

To describe the interaction between different molecules and atoms, specific potential models are used. The interaction force can be calculated as the negative derivative of the potential model. In this study, we use the following shifted Lennard-Jones 12–6 potential [10] to

\*Corresponding author. Email: cfdai0421@gmail.com

Table 1. Intermolecular potential models and parameters used in this study.

Particle groups	Potential model	Parameters
Fluid particles (CH <sub>3</sub> , CH <sub>2</sub> ), Wall particles (Au)	$U_S(r) = \begin{cases} U_{LJ}(r) - U_{LJ}(r_c) - [r - r_c](dU_{LJ}/dr)r_c & r \leq r_c \\ 0 & r > r_c \end{cases}$ $U_{LJ} = 4\epsilon \left[ \left( \frac{\sigma}{r_{ij}} \right)^{12} - \left( \frac{\sigma}{r_{ij}} \right)^6 \right]$	$\sigma_{CH_2-CH_2} = 0.387 \text{ nm}$ $\sigma_{CH_2-CH_3} = 0.387 \text{ nm}$ $\epsilon_{CH_2-CH_2} = 88.0 \text{ K}$ $\epsilon_{CH_2-CH_3} = 59.38 \text{ K}$ $\epsilon_{CH_3-Au} = 5132 \text{ K}$ $\epsilon_{CH_2-Au} = 5132 \text{ K}$
Wall particles	$U_{\text{nonlinear}} = \frac{H_1}{2}R^2 + \frac{H_2}{4d_{\text{cr}}^2}R^4 + \frac{H_3}{6d_{\text{cr}}^4}R^6,$	$H_1 = 57, H_2 = 20, H_3 = 50$

model the inter-molecular interaction:

$$U_S(r) = \begin{cases} U_{LJ}(r) - U_{LJ}(r_c) - [r - r_c](dU_{LJ}/dr)r_c & r \leq r_c \\ 0 & r > r_c \end{cases}$$

and

$$U_{LJ} = 4\epsilon \left[ \left( \frac{\sigma}{r_{ij}} \right)^{12} - \left( \frac{\sigma}{r_{ij}} \right)^6 \right],$$

where  $\epsilon$  represents the binding energy,  $\sigma$  the equilibrium distance between two atoms,  $r_{ij}$  the distance between two atoms and  $r_c$  the cut-off radius (set as  $2.5\sigma$  in this study to

reduce computational time). The shifted Lennard-Jones 12-6 potential is adopted to model the interaction between metal wall particles and propane molecules, but is used with different parameters [11]. The parameters for different particle groups, which are obtained from the Lorentz-Berthelot mixing rule [12], are  $\sigma_{ij} = (\sigma_{ii} + \sigma_{jj})/2$  and  $\epsilon_{ij} = \sqrt{\epsilon_{ii}\epsilon_{jj}}$ . To describe the vibrations of liquid propane molecules, the harmonic potential functions [13] are used. Each propane molecule contains three sites: one CH<sub>2</sub> site and two CH<sub>3</sub> sites. The equilibrium values for the carbon-carbon bond length and the C-C-C bond angle are 1.526 Å and 112.4°, respectively. The parameters used for harmonic potential are 96,500 K/Å<sup>2</sup> and 62,500 K/rad<sup>2</sup> for bond stretching and bond bending, respectively.

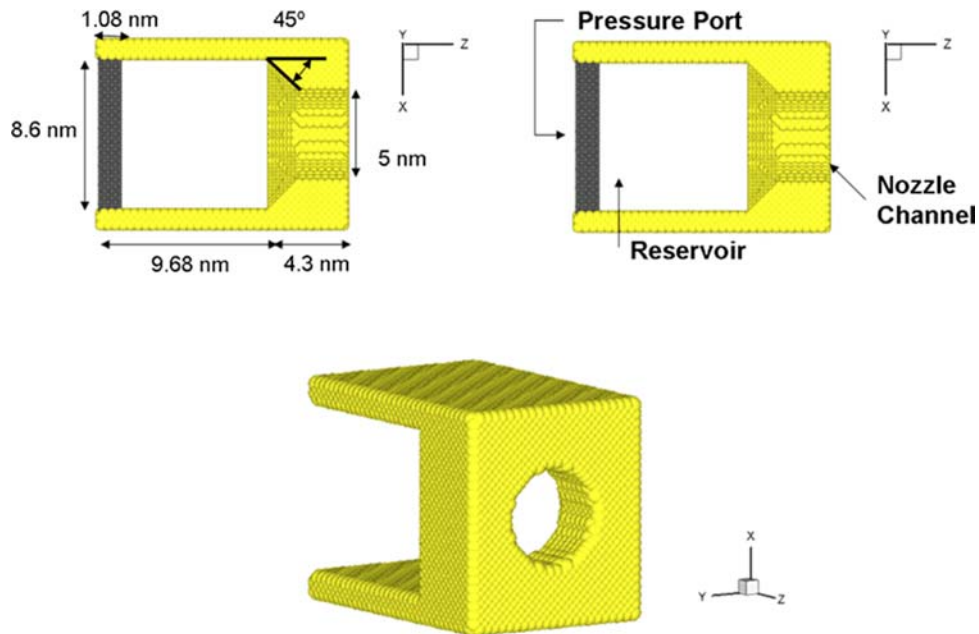


Figure 1. The geometry and size of the nanojet system.

Atoms in the solid walls oscillate from their initial lattice sites. To simulate this thermal fluctuation of metal particles, we employed the non-linear spring potential model [14]; the potential is listed below:

$$U_{\text{nonlinear}} = \frac{H_1}{2}R^2 + \frac{H_2}{4d_{\text{cr}}^2}R^4 + \frac{H_3}{6d_{\text{cr}}^4}R^6,$$

where  $H_1$ ,  $H_2$  and  $H_3$  are the parameters of the non-linear spring potential;  $R$  is the displacement of particle position from the original lattice position. The critical displacement of lattice position  $d_c$  is set as 0.0025 times the lattice length. All the simulation models and parameters used in this study are listed in Table 1.

The temperature of the nozzle, which was made of gold, is controlled by the velocity scaling method [10], which is described below.

$$v_i^{\text{new}} = v_i \sqrt{\frac{T_D}{T_A}},$$

where  $T_A$  represents the actual temperature of the system,  $T_D$  the desired temperature of the system,  $v_i$  the original velocity of the atoms and  $v_i^{\text{new}}$  the modified velocity of the atoms. Before ejection, the temperature of the fluid molecules is controlled by the Nose–Hoover [15] thermostat,

$$\begin{aligned} v_i &= p_i/m_i, \\ \dot{p}_i &= F - \varsigma \cdot p_i, \quad \text{and} \\ Q\dot{\varsigma} &= \sum_i p_i^2/m_i - gkT_D, \end{aligned}$$

where  $p_i$  represents the momentum of the atoms,  $\dot{p}_i$  the acceleration and  $m_i$  the mass. The values of the parameters  $\varsigma$  and  $Q$  of the thermostat method are chosen as 10 time step and the triple of system mass, respectively. The integral time interval in this study is about 1 fs and the equation of motion is integrated by a fifth-order Gear predictor–corrector method [10].

The geometry of the simulation system is illustrated in Figure 1. The nozzle system is surrounded by a vacuum environment. The entire nozzle is constructed by a FCC lattice and in total contains 29,090 Au atoms, which include the pressure port, reservoir and the nozzle channel. The diameter of the nozzle channel is 5 nm. The total nozzle system is about 14 nm long and 9 nm wide. The fluid reservoir contains 6000 initially random propane molecules that are contained in an 8.6 nm × 8.6 nm × 8.98 nm reservoir. A plate placed behind the reservoir functions as a pressure port and contains in total 5412 Au atoms. Ejection occurs when this plate is used to propel the fluid molecules into the nozzle channel at a constant velocity.

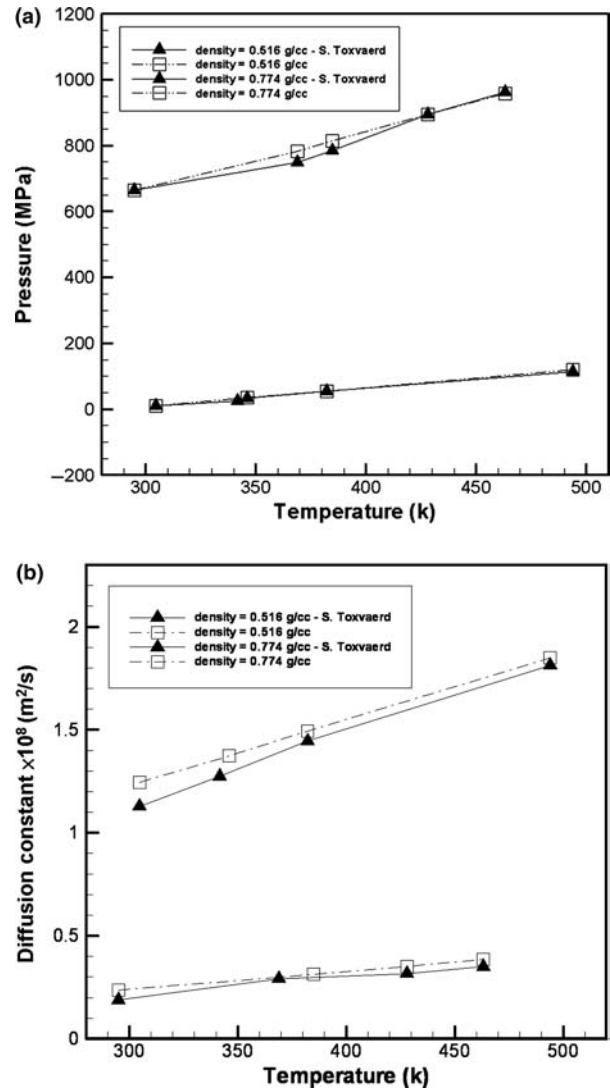


Figure 2. (a) The pressure versus temperature plot of propane molecules of different densities. The reference data are from [13]. (b) The diffusion constants of propane molecules under various conditions. The reference data are from [13].

The initial temperature for the wall and fluid molecules is 150 K, and the solid wall temperature is kept at 150 K throughout the simulation. To avoid any skewing of the results by any non-ideal conditions present during the preparation period, all the simulation results used to obtain average values are gathered after the system has reached equilibrium. When it reaches the thermal equilibration, the equilibrium temperature is 150 K and pressure is about 500 MPa. A long period of time is necessary to reach thermal equilibrium between the wall and fluid atoms; the equilibration time is related to the set-up of the initial condition. In this study, the system reaches equilibrium after 100,000 time-steps.

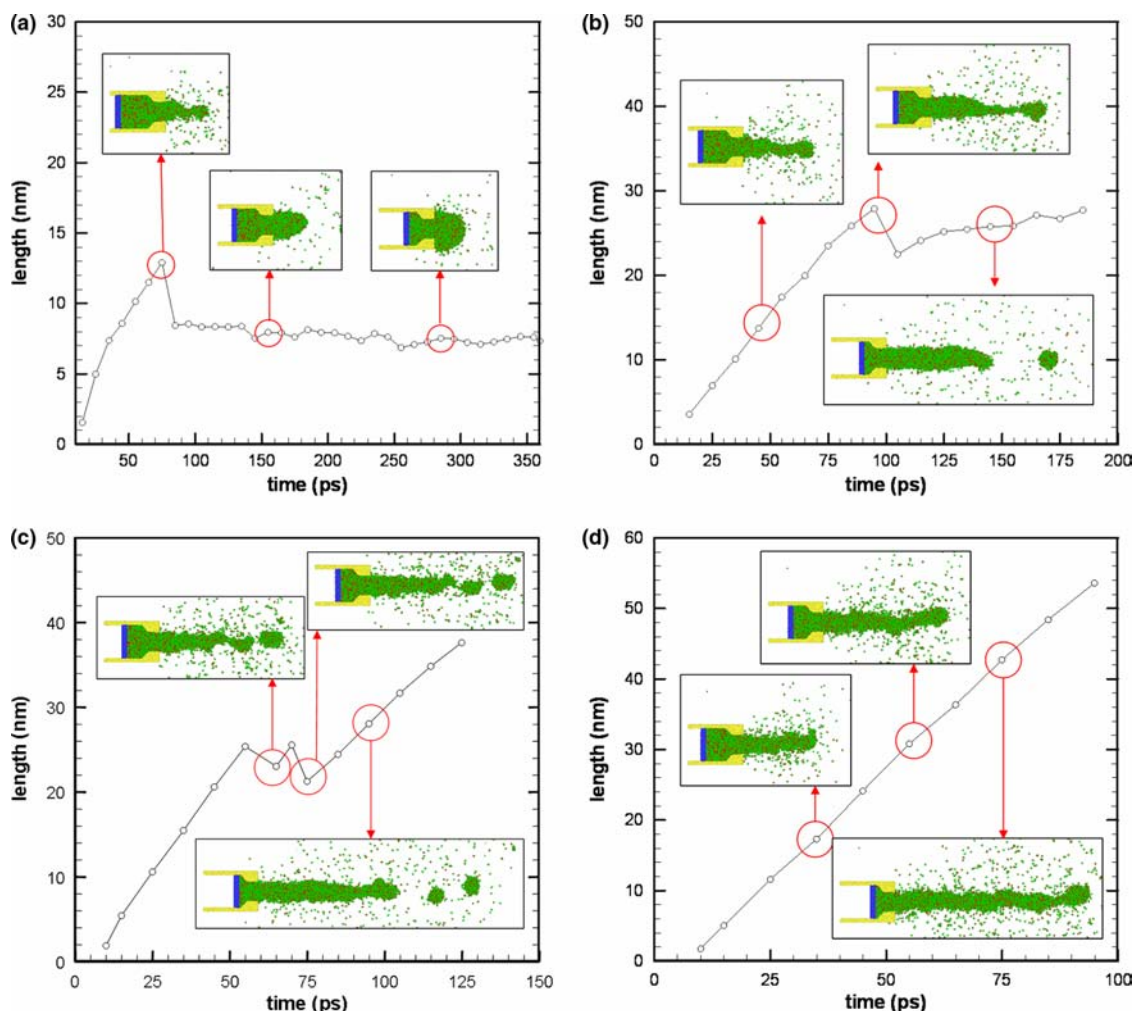


Figure 3. A snapshot of the ejection process and length of liquid thread evolution for various compressing velocities: (a) 22 m/s. (b) 44 m/s. (c) 66 m/s and (d) 88 m/s.

### 3. Results and discussion

To confirm the accuracy of the potential model and the method used in this study, using MD simulation we calculate the pressure values for liquid propane at various temperatures and densities. The diffusion constant in various states is also calculated. The periodic boundary conditions [10] are applied in the  $x$ -,  $y$ - and  $z$ -directions to obtain the bulk properties. All simulation results are gathered to calculate average values after the system reaches equilibrium. The results are shown in Figure 2(a),(b) and are found to be in good quantitative agreement with the results of related investigations [13]. This supports the accuracy of the simulation models and methods used in this work.

#### 3.1 Ejection process results for various compressing velocities

To investigate the influence of the compressing velocity on fluid molecules in nanojet processes, we set four different

compressing velocities in the range of 22–88 m/s: 22, 44, 66 and 88 m/s. The compressing plate is set to move the same total distance in each case, each run broken up into 25 time steps that are equal within the run. Snapshots of the ejection process for the various cases are presented in Figure 3. In this figure, the  $\text{CH}_3$  particles of propane molecules are green, the  $\text{CH}_2$  particles of propane molecules are red, the wall molecules are yellow and the pressure port molecules are blue. The break-up profiles tend to resemble the double-cone structure which is also found in related research [4]. The simulation results for various compressing velocities show that the lengths of liquid threads are strongly dependent on the compressing velocity.

In the case of the lowest compressing velocity (22 m/s), shown in Figure 3(a), the propane molecules finally assemble into a semi-sphere droplet and are adsorbed on the exterior of the nozzle wall. Obviously, this is because the inertia force of fluid molecules is not high



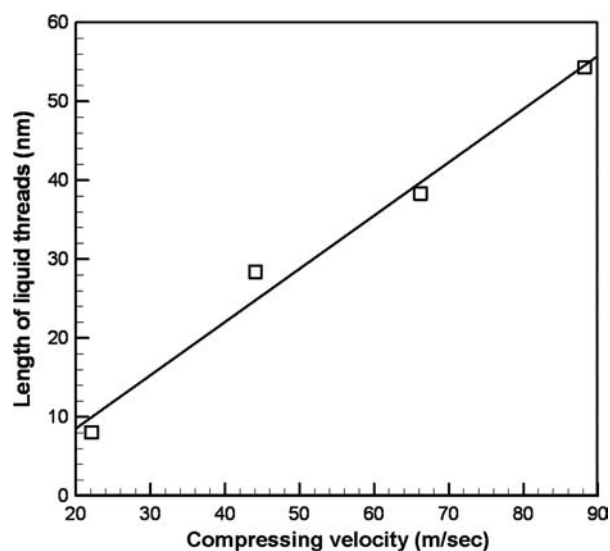


Figure 4. Final lengths of liquid threads for various compressing velocities.

enough to overcome the adsorption force of interaction between the nozzle atoms and the fluid molecules. Therefore, the liquid thread cannot hold a cylindrical shape.

The nanojet ejection results for higher compressing velocities are shown in Figure 3(b)–(d). As the compressing velocity increases, the length of the liquid threads tends to increase as well. This is because the system energy increases when the compressing plate does work on the fluid molecules. This gives the fluid molecules more kinetic energy to overcome the adsorption on the nozzle surface and remain in a cylindrical shape. However, it can also be shown that higher kinetic energy increases the amount of evaporation and the instability of the cylindrical shape. This could result in irregular fracture and produce more satellite droplets.

Investigation of the lengths of the liquid threads produced at various compressing velocities show that they increase with time. The sharp peak shows that the first break-up for all the different cases happens somewhere in the range of 50–100 ps. The break-up times of the cases with lower compressing velocities (22 and 44 m/s) are close to each other and are of the order of 100 ps. Since the system has higher kinetic energy in the case with the higher compressing velocity of 66 m/s, the threads are more unsteady; a short break-up time (55 ps) and a second break-up are seen. Furthermore, for the case with the highest compressing velocity (88 m/s), the phenomenon of break-up does not occur until the end of the simulation. According to the Rayleigh instability theory [3], which has been shown to be valid at the nanoscale [16], a thread is unstable and shall break-up into droplets if  $L > 2\pi R$ , where  $L$  is the length of the

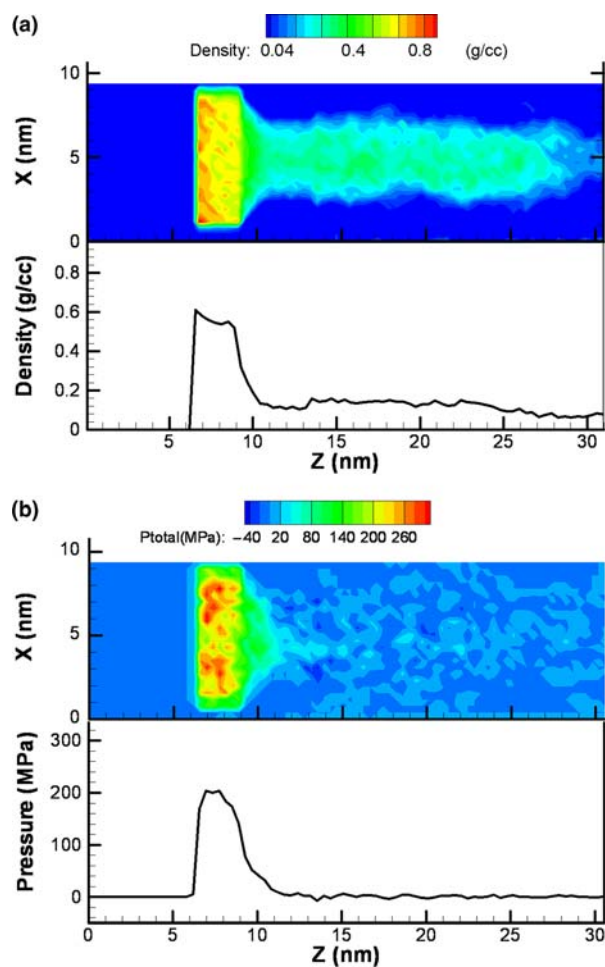


Figure 5. (a) Density and (b) pressure distributions for nanojet process at 120 ps. The compressing velocity is 44 m/s.

thread and  $R$  is the radius of the cylindrical liquid jet. This would be attributable to the total ejection process, in this case being too short. The surface energy cannot cause the propane molecules to assemble into a double-cone break-up structure until the end of simulation; therefore, the thread does not break-up. To confirm this opinion, the same ejection system with longer simulation time is performed. The result shows that the break-up happened at about 100 ps in this case. Therefore, the timing for propagating surface energy played an important role for thread break-up. The Rayleigh instability is still applicable for this study.

Minor recoiling phenomena are seen after the thread break-up for the case of a compressing velocity of 22 m/s. In the other cases, the systems contain high enough energy that the lengths of the threads continue increasing as the plate compresses.

The final lengths of liquid threads for various compressing velocities are shown in Figure 4. The break-up positions tend to linearly increase with the

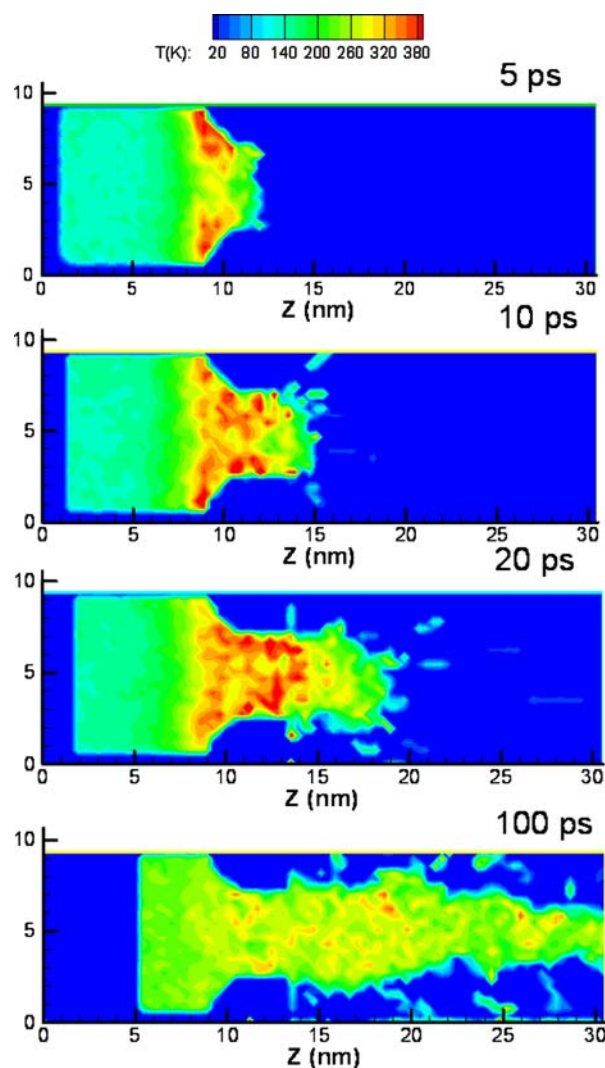


Figure 6. Temperature distribution for the nanojet process. The compressing velocity is 44 m/s.

compressing velocity. This study found a linear relationship between the compressing velocity and the thread length for velocities between 22 and 88 m/s. This information can help us to determine the appropriate distance between nozzle and manufacturing surface.

### 3.2 Property distribution and energy

To analyse the ejection process in greater detail, density and pressure distributions for a compressing velocity of 44 m/s at 120 ps are shown in Figure 5(a),(b). The layer density distribution in Figure 5(a) shows that the density is neither uniform nor continuous at the nanoscale. Local maximum high-density regions of approximately 0.6 g/cc appeared near the pressure port. Figure 5(b) shows the pressure distribution. Similar to the density distribution,

local high-pressure regions appear near the pressure port. After propane molecules eject from the nozzle, the pressures reduce rapidly and finally tend to zero. This is because the nozzle system is surrounded by a vacuum environment. Along the axis of the nozzle outlet, both density and pressure decrease farther away from the outlet. These results suggest a mechanism whereby the fluid molecules are compressed by the pressure port and form high-pressure regions. After pressure propagation, the high pressure is released and the fluid molecules are ejected through the nozzle.

Figure 6 shows the temperature distribution at the beginning of the ejection process. The fluid temperature is not constant during this process. As the plate compresses, high-temperature regions appear in the contracting part of the nozzle channel. It is obvious that shear heating phenomena occurred along the region of contact. This shows that the shear heating may influence the ejection process at the nanoscale. By heat conduction and convection, the temperature distribution becomes more uniform as the ejection process continues.

Figure 7(a)–(d) shows the energy evolution of ejection processes for various compressing velocities. The total energy includes both kinetic energy and Lennard-Jones potential energy. The results show that the energy terms increase with time. For the cases with lower compressing velocities (Figure 7(a),(b)), the total energy profiles are similar to the Lennard-Jones energy. By contrast, for the cases with higher compressing velocities, the total energy profiles are similar to the kinetic energy (Figure 7(c),(d)). This is because the velocity of fluid molecules increases with that of plate compression. As a result, for the cases with higher compressing velocities, the kinetic energy term undergoes a greater increase than the potential energy. The Lennard-Jones energy in Figure 7(c),(d) shows that the fluid molecules have higher energy levels than those in Figure 7(a),(b). As a result, irregular fracture and an increase in the occurrence of satellite droplets are expected. The higher kinetic energy also increases the number of evaporating molecules and satellite droplets.

## 4. Conclusion

Non-equilibrium MD was used in this study to simulate nanojet processes involving the compression of liquid propane into the nozzle channel using various velocities for the compressing plate; the results of these simulations have been presented and discussed in this paper.

Properties' distributions show that the density and pressure are neither uniform nor continuous at the nanoscale during the ejection process. Local high-pressure regions appear near the pressure port. As the plate compressed, shear heating phenomena occurred in

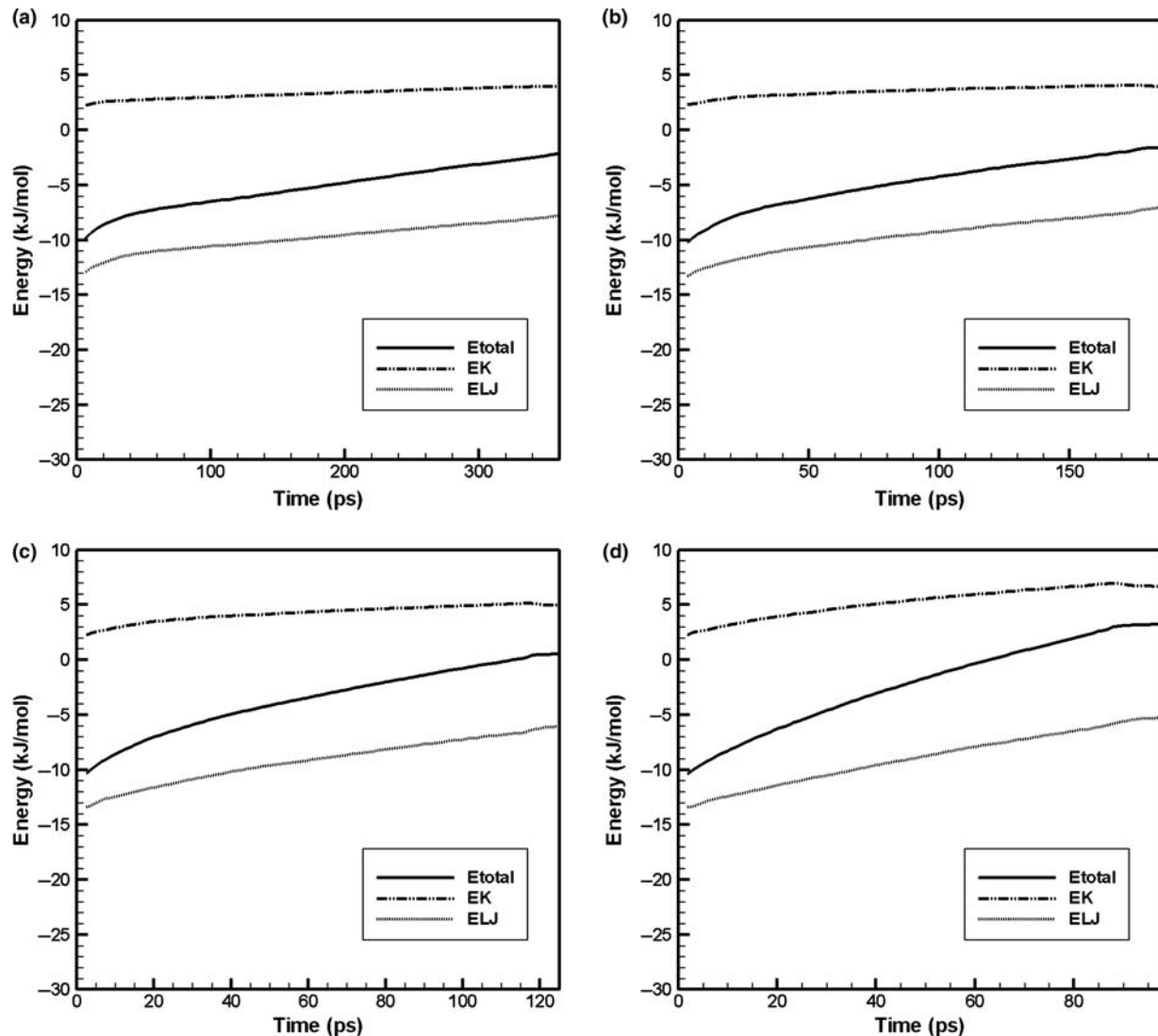


Figure 7. Results for the time evolution of the energy change for compressing velocities of (a) 22 m/s. (b) 44 m/s. (c) 66 m/s and (d) 88 m/s.

the region of contact with the nozzle channel. The length of the liquid threads tended to increase along with the compressing velocity. A linear relationship between the length of the liquid threads and the compressing velocity was found. A higher compressing velocity also led to a higher energy level in the system; this increased the amount of evaporation and the instability of the cylinder structure. This could result in irregular fracture and produce more satellite droplets.

### Acknowledgements

The authors thank the National Science Council of the R.O.C. for partially supporting this research under contract no. NSC 95-2221-E-007-082.

### References

- [1] F. Korte, J. Koch, J. Serbin, A. Ovsianikov, and B.N. Chichkov, *Three-dimensional nanostructuring with femtosecond laser pulses*, IEEE Trans. Nanotech. 3 (2004), pp. 468–472.
- [2] M. Gad-el-Hak, *MEMS: Applications*, CRC Press, Boca Raton, 2005.
- [3] J. Eggers, *Nonlinear dynamics and break-up of free-surface flows*, Rev. Mod. Phys. 69 (1997), pp. 865–929.
- [4] U. Landman and M. Moseler, *Formation, stability, and break-up of nanojets*, Science 289 (2000), pp. 1165–1169.
- [5] W. Kang and U. Landman, *Universality crossover of the pinch-off shape profiles of collapsing liquid nanobridges in vacuum and gaseous environments*, Phys. Rev. Lett. 98 (2007), 064504.
- [6] J. Eggers, *Dynamics of liquid nanojets*, Phys. Rev. Lett. 89 (2002), 084502.
- [7] Y.S. Choi, S.J. Kim, and M.U. Kim, *Molecular dynamics of unstable motions and capillary instability in liquid nanojets*, Phys. Rev. E 73 (2006), 016309.



- [8] K. Ichiki and S. Consta, *Disintegration mechanisms of charged aqueous nanodroplets studied by simulations and analytical models*, J. Phys. Chem. B 110 (2006), pp. 19168–19175.
- [9] S. Murad and I.K. Puri, *Nanoscale jet collision and mixing dynamics*, Nano Lett. 7 (2007), pp. 707–712.
- [10] J.M. Haile, *Molecular Dynamics Simulation: Elementary Method*, John Wiley & Sons, New York, 1997.
- [11] D.C. Rapaport, *The Art of Molecular Dynamics Simulation*, Cambridge University Press, Cambridge, 1995.
- [12] A.K. Al-Matar and D.A. Rockstraw, *A generating equation for mixing rules and two new mixing rules for interatomic potential energy parameters*, J. Comput. Chem. 25 (2004), pp. 660–668.
- [13] S. Toxvaerd, *Molecular dynamics calculation of the equation of state of liquid propane*, J. Chem. Phys. 91 (1989), pp. 3716–3720.
- [14] X.J. Fan, N. Phan Thien, N.T. Yong, and X. Diao, *Molecular dynamics simulation of a liquid in a complex nano channel flow*, Phys. Fluids 14 (2002), pp. 1146–1153.
- [15] S. Nosé, *A unified formulation of the constant temperature molecular dynamics methods*, J. Chem. Phys. 81 (1984), pp. 511–519.
- [16] D. Min and H. Wong, *Rayleigh's instability of Lennard-Jones liquid nanothreads simulated by molecular dynamics*, Phys. Fluids 18 (2006), 024103.